



ELECTROSTATIC ACCELERATORS OF IPPE FOR NUCLEAR SCIENCE AND TECHNOLOGY

Gulevich A.V.*, Birzhevoy G.A., Glotov A.I., Gurbich A.F.,
Zhdanov G.S., Konobeyev Yu.V., Kostrigin N.A., Kuzminov B.D.,
Pechenkin V.A., Plaksin O.G., Romanov V.A., Rykov V.A.,
Fursov B.I., Zrodnikov A.V.

**International Topical Meeting on Nuclear
Research Applications and Utilization of
Accelerators**

4 to 8 May 2009, Vienna, Austria





ELECTROSTATIC ACCELERATORS OF IPPE



Ion energy range	- 0.1...60	MeV
Ion current	- 0.01...2500	μA
Ion mass range	- 1...60	a.m.u

ELECTROSTATIC ACCELERATORS OF IPPE

TYPE OF ACCELERATOR	ENERGY FOR SINGLE-CHARGED IONS MeV	ACCELERATED IONS	CONTINUOUS/ /PULSE BEAMS	BEAM INTENSITY
EG-2,5	0,2...2,5	H, D	CONTINUOUS	0,1...50 μ A
		He, N, Ar, O		0,01...10 μ A
EG-1	0,9...4,5	H, D	CONTINUOUS	1,0...30 μ A
			PULSE	2...3 mA $T_{h/2} - 1...2$ ns frequency - 1...5 MHz
EGP-10M	3,5...9,5	H, D	CONTINUOUS	0,01...10 μ A
			PULSE	400 μ A $T_{h/2} - 1$ ns frequency - 1...5 MHz
KG-2,5	2,3	H, D	CONTINUOUS	0,05...2,0 mA
KG-0,3	0,35	H, D	CONTINUOUS	1,0...2000 μ A
			PULSE	2...3 mA $T_{h/2} - 1...3$ ns frequency - 0,5...2,5 MHz
EGP-15	13	H, D	CONTINUOUS	5 μ A
			PULSE	400 μ A $T_{h/2} - 1$ ns frequency - 1...5 MHz
		C, Li, O, Al, Si, Cl, Fe, Ni, Cu, Zr	CONTINUOUS	0,01...1,0 μ A

Main directions of scientific research on electrostatic accelerators of IPPE

- **Nuclear physics of low and intermediate energies. Nuclear data for nuclear power engineering. Closed nuclear fuel cycle. Safe management and disposition of radioactive wastes and spent nuclear fuel.**
- **Solid-state physics. Physics of radiation damage and material irradiation studies.**
- **Nuclear micro-analysis. Analysis of material structure and composition.**
- **Physics of nuclear-excited dust plasma. Direct conversion of nuclear energy in nuclear-pumped lasers.**
- **Activation analysis. Wear and corrosion monitoring by surface activation method.**
- **Beam technologies. Nanotechnologies and nanomaterials.**
- **Technologies for manufacturing membranes and catalytic systems. Technologies of hydrogen energy.**

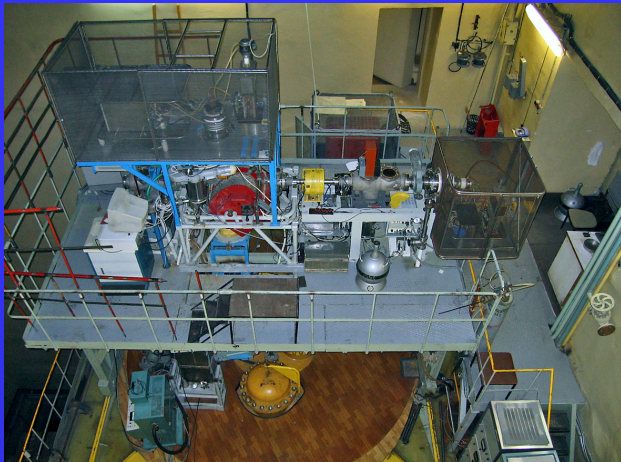
Nuclear physics of low and intermediate energies

The following measurements have been fulfilled on the accelerator complex:

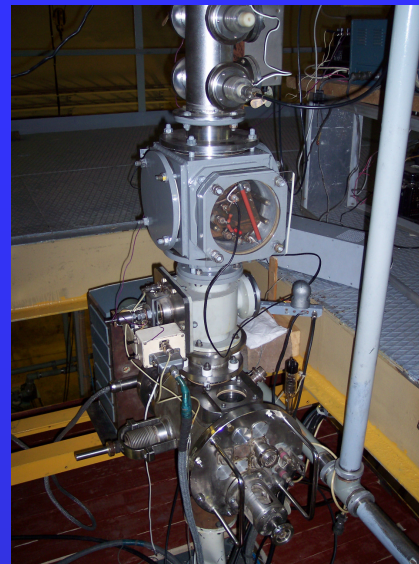
- fission cross-sections in the range of neutron energies of 0 - 7 MeV for the Th-232, Pa-231 nuclei, for all uranium isotopes from 232 to 238, for Np-237, for all isotopes of plutonium, from 238 to 243, all isotopes of curium, from 243 to 248, and for Cf-249
- the multiplicity of prompt neutrons in nuclear fission by neutrons in the energy range up to the threshold of 6MeV for Th-232 , U-233,-235,-236,-238, Np-237
- cross-sections and spectra of neutrons in reactions (n,n') , $(n,2n)$, and (n,f) for a wide scope of nuclei from Li-6 to Np-237
- cross-sections of radiative capture of neutrons for nuclei of structural materials, nuclei-fission products, and several fissionable nuclides
- yields of delayed neutrons and their dependence on the energy of neutrons which cause fission of Th-232, U-235, U-238, Pu-239, Np-237, Am-243 nuclei.

Physics of radiation damage and radiation materials science

ANALYTICAL MATERIAL IRRADIATION STUDY COMPLEX BASED ON ELESTROSTATIC ACCELERATOR EGP-15



Injector of light and heavy ions of accelerator



*Irradiation camera
12 samples can be irradiated simultaneously*



Horizontal ion guide of EGP-15 accelerator

Electrostatic accelerator EGP-15 allow to obtain the ion beams for the most part of elements in Mendeleev's Periodic Table. For the simulation research beams of accelerated ions of nickel and zirconium are required in many cases.

After the modernization the ion beam intensity amounts to: $\text{Ni}^{+2} - 0.5 \mu\text{A}$; $\text{Ni}^{+3} - 0.4$; $\text{Zr}^{+2} - 0.2 \mu\text{A}$.

A system of accelerated ions' distribution density control over the beam cross-section in the course of irradiation has been developed and applied. To ensure an even irradiation of entire surface of the sample, the method of beam sweeping in the irradiation plane with electrostatic correctors is used. Estimated non-uniformity of the beam $< 10\%$.

MAIN DIRECTIONS OF ROSATOM'S PROGRAM FOR NEW MATERIALS BASED ON THE USE OF SIMULATION TECHNOLOGIES:

1. Fast reactors (BN-600, BN-800, BN-1800):

- materials of fuel pin claddings, to achieve the burn-up of 11 % U and the damaging dose up to 90 dpa – modified austenitic steel ChS68 c.w.;
- materials of claddings, to achieve the burn-up of 15 % U and the damaging dose up to 140 dpa - austenitic steel EK164 c.w. and ferritic-martensitic steels EK181 and ChS139;
- materials of claddings, to achieve the burn-up of 17-18 % U and the damaging dose up to 180 dpa – oxide-dispersive-strengthened ferritic-martensitic steels;

2. Thermal neutron reactors (VVER (PWR) and RMBK (BWR)):

- modified zirconium alloys E110M and E635M, achieve the burn-up of 75-80 MW day/kg U.

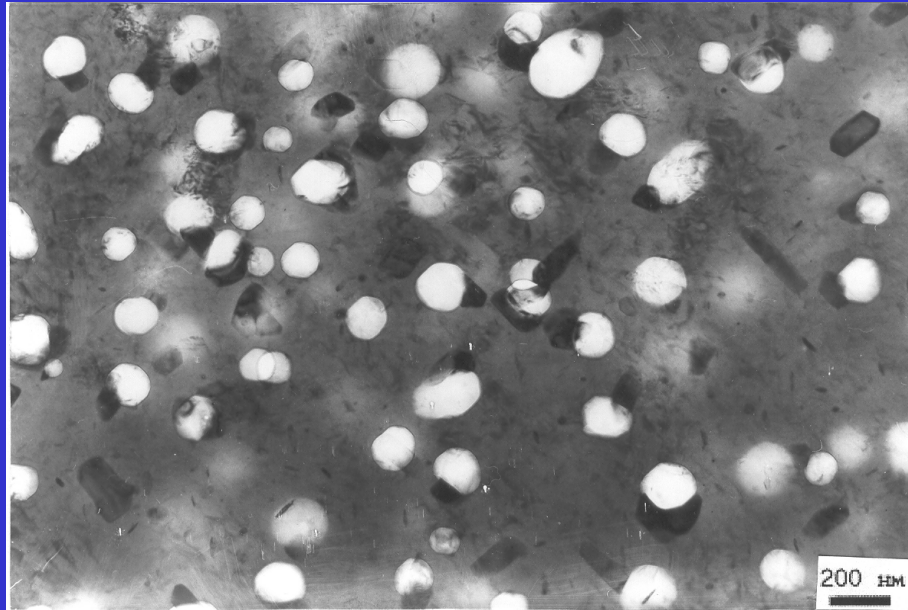
3. Fusion reactors:

- surface erosion,
- swelling,
- modification of structure.

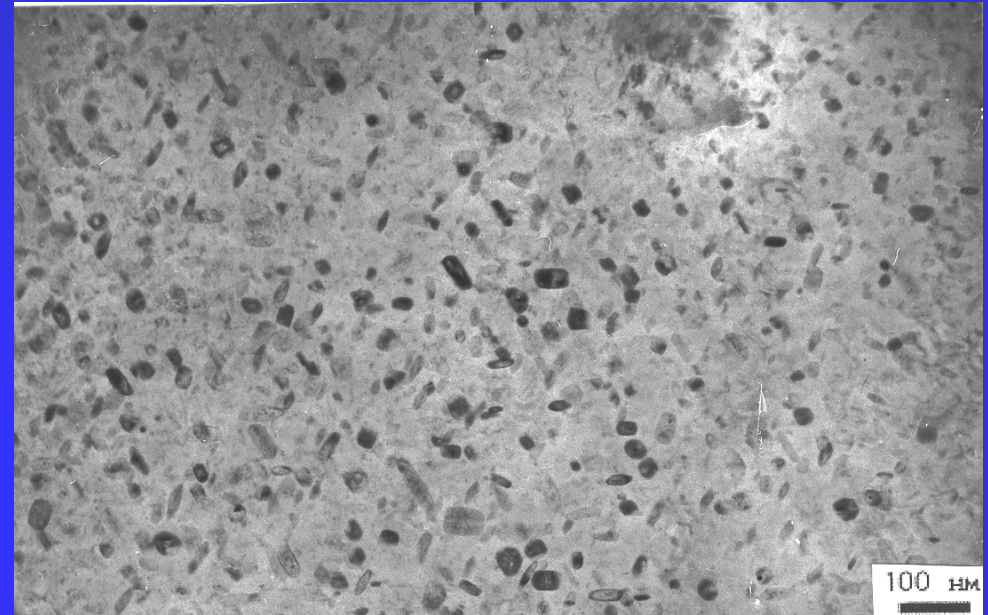
PRINCIPAL PROBLEMS OF SIMULATION TECHNOLOGIES:

1. **Austenitic steels – effects of impurity and alloying elements and technology of fabrication on swelling (fluence and temperature dependencies);**
2. **Ferritic-martensitic steels – effects of impurity and alloying elements and technology of fabrication on swelling (at high damaging doses) and the structure in the range of low-temperature radiation embrittlement (fluence and temperature dependencies);**
3. **Oxide-dispersive-strengthened (ODS) steels – stability of oxides under irradiation;**
4. **Zirconium alloys - effects of impurity and alloying elements and technology of fabrication on the corrosion resistance and structure.**

Ions used in simulation experiments: protons, helium, heavy ions



a)

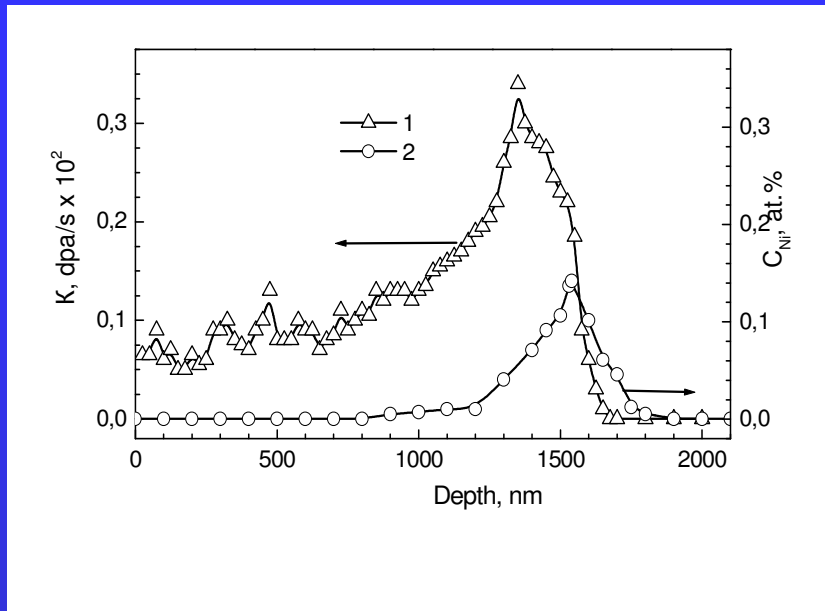


b)

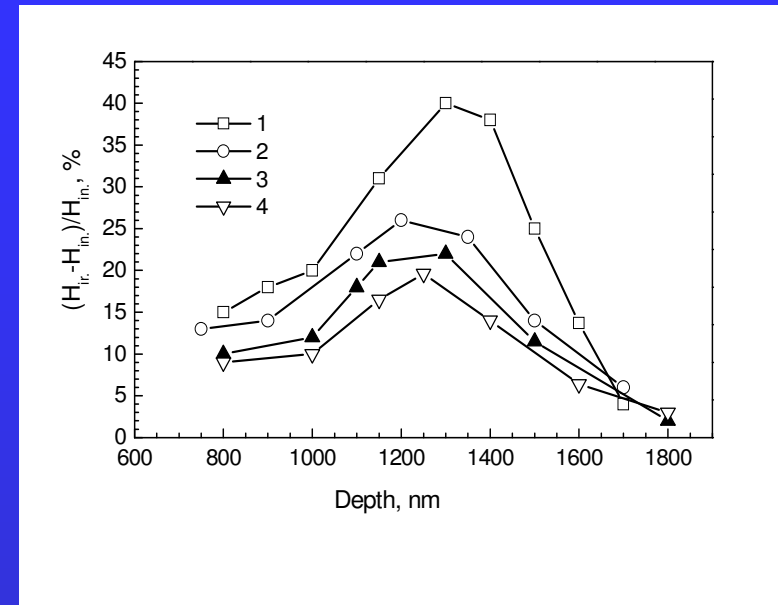
Vacancy pores (voids) in Cr18Ni9Ti steel (a) and fine-dispersed TiC and G-phase precipitates in EK-164 c.w. steel (b) after irradiation by 7 MeV Ni⁺⁺ ions to 30 dpa at 625° C

Radiation-induced segregation

Since there is a correlation between the microhardness values and yield strengths in both ferritic and austenitic steels, the measurements of microhardness allow studying of the radiation-induced hardening in materials after ion irradiation



a) Profiles of the distribution of radiation damage formation rate (1) over depth and implanted ions of nickel (2) with energy $E = 7$ MeV on the accelerator EGP-15 (at $\Phi=10$ dpa)



b) Distribution of relative changes of microhardness near the surface of steel EP-823 under similar irradiation conditions at different temperatures 1 - 380, 2 - 450, 3 - 550, 4 - 600 °C

Radiation-induced segregation

- **Radiation-induced segregation (RIS) results in a considerable change in the alloy composition near the main objects of microstructure: the grain boundaries and sample surface, dislocations, precipitates, voids and gas bubbles, and it strongly affects the phase composition, swelling, corrosion, embrittlement and other radiation phenomena in structural materials**
- **Accelerators also make it possible to fulfill in parallel the studies of RIS near the sample surface in these materials. The investigations have covered V-Fe and Fe-Cr alloys, ferritic-martensitic steel EP-823 irradiated in ILU-100 and EGP-15 accelerators.**
- **The data on RIS in alloys near the sample surface obtained in the ion irradiation can be used in the modeling of RIS in these alloys near other microstructure objects, as well as for other irradiation conditions. Therefore, the heavy ion irradiation of advanced structural materials is an informative express-method for studies of radiation-induced segregation in these materials.**

Accelerator testing of materials in-situ

Most relevant approach

“**during irradiation**” is more than “**before + after irradiation**”

Dynamic and transient radiation-induced effects

Structural: recrystallization, phase transitions

Electrical: conductivity (RIC), charging, RIEMF

Optical: photon emission, transient absorption

Mechanical: creep, swelling, etc.

Advantages of accelerators (vs. reactors)

- variety of methods of in-situ testing
- facile simultaneous measurements → correlations
- controllability in experiments
- lower costs on testing

Materials

Structural: Vanadium, zirconium, chromium-nickel alloys, SiC

Insulators: oxide and nitride ceramics

Optical: oxide and fluoride single crystals and glasses

Tasks

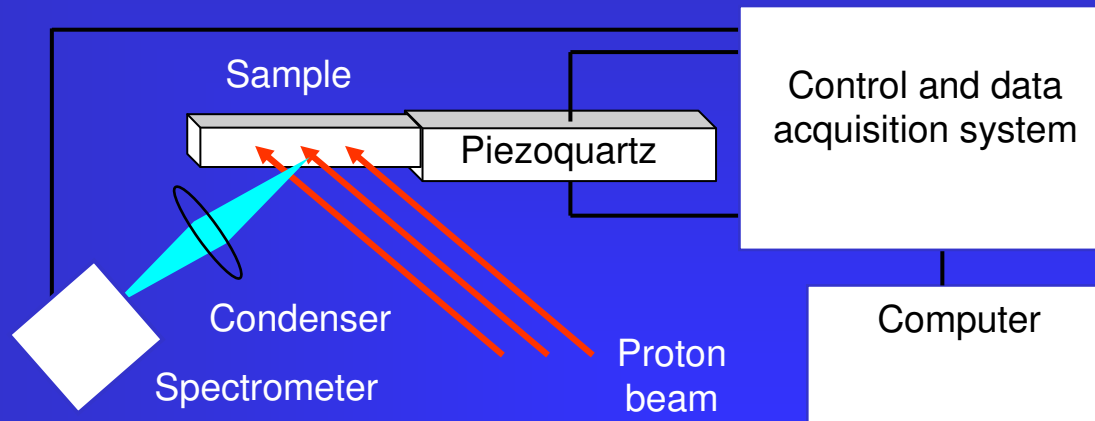
ITER Engineering Design Activity

New-Generation Fast Fission Reactors

Nuclear-Pumped Lasers

Nanotechnologies

Acoustic-optical method in-situ



EGP-15 accelerator:

Protons

Energy 10 MeV

Current density $0.3 \mu\text{A}/\text{cm}^2$

(Dose rate 16 kGy/s)

Spectrometer:

Wavelength 400-700 nm

Composite oscillator:

Frequency 102 kHz

Strain amplitude $10^{-6} - 10^{-4}$

Simultaneous measurements:

Young modulus

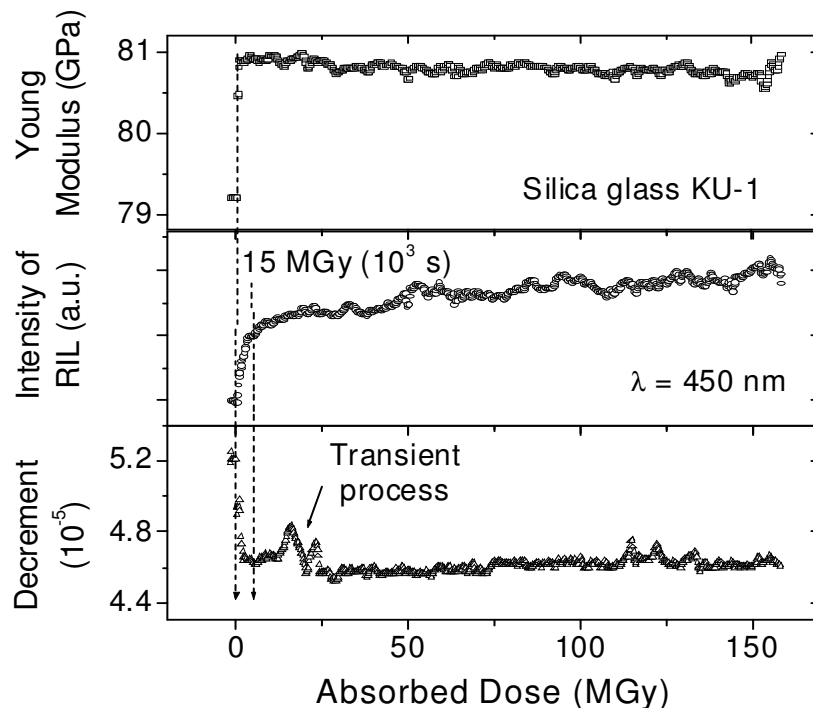
Decrement of ultrasonic vibration

Strain amplitude

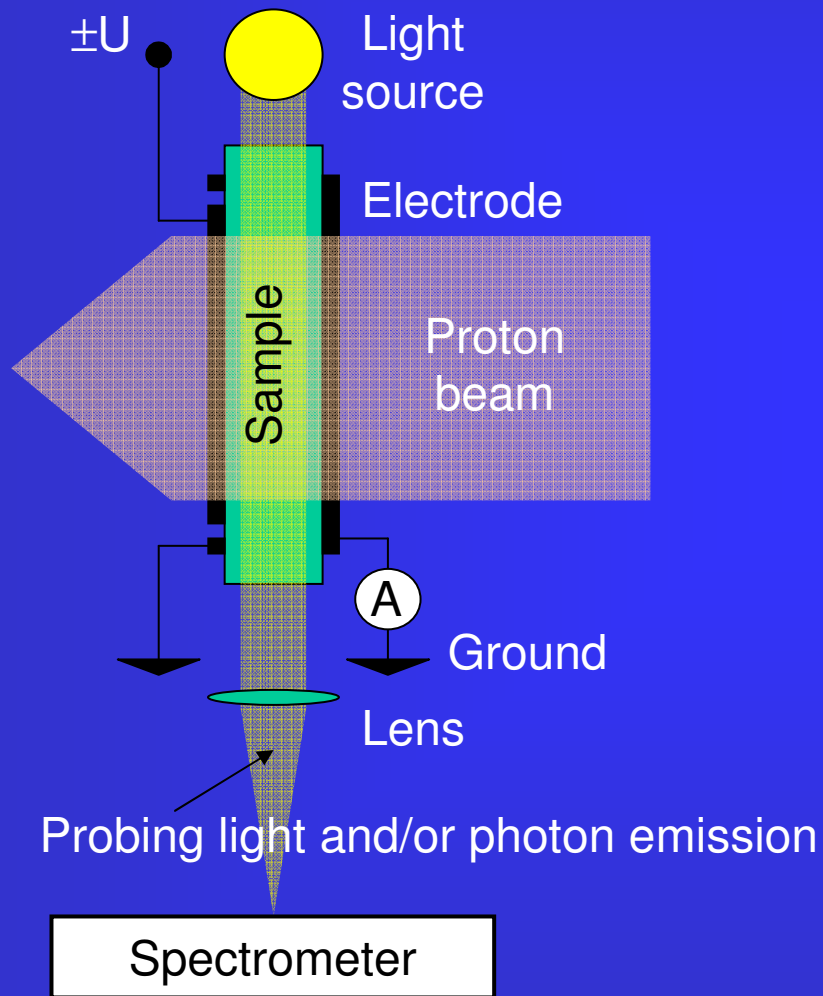
Radioluminescence (RIL)

Proton flux

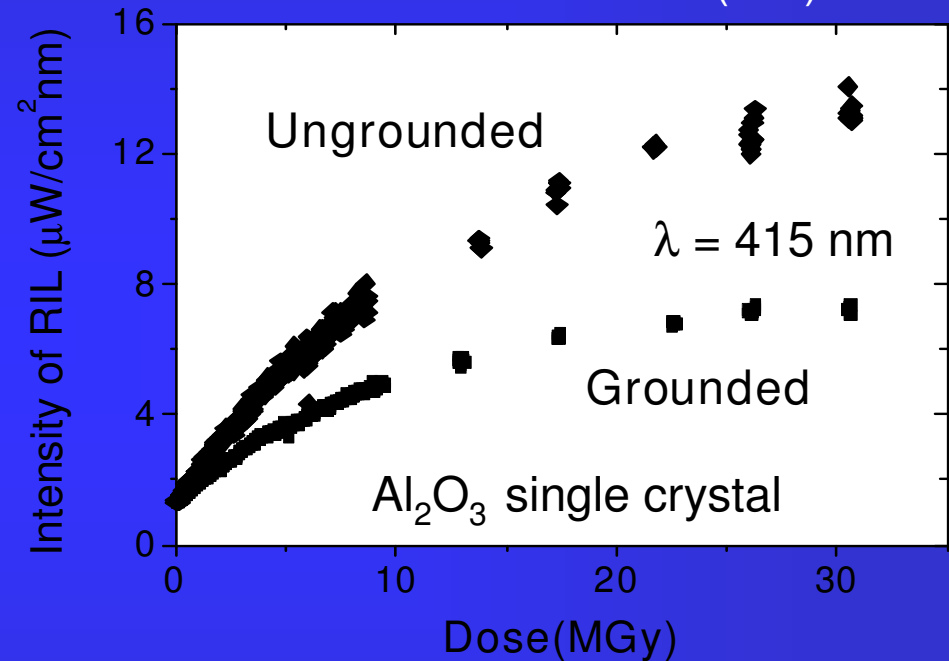
Temperature of sample



Radiation testing of materials in-situ: Electrical and optical properties



Effect of electrical charging on radioluminescence (RIL)



Simultaneous measurements:
Radiation-induced conductivity
Radioluminescence
Radiation-induced optical absorption
Proton flux

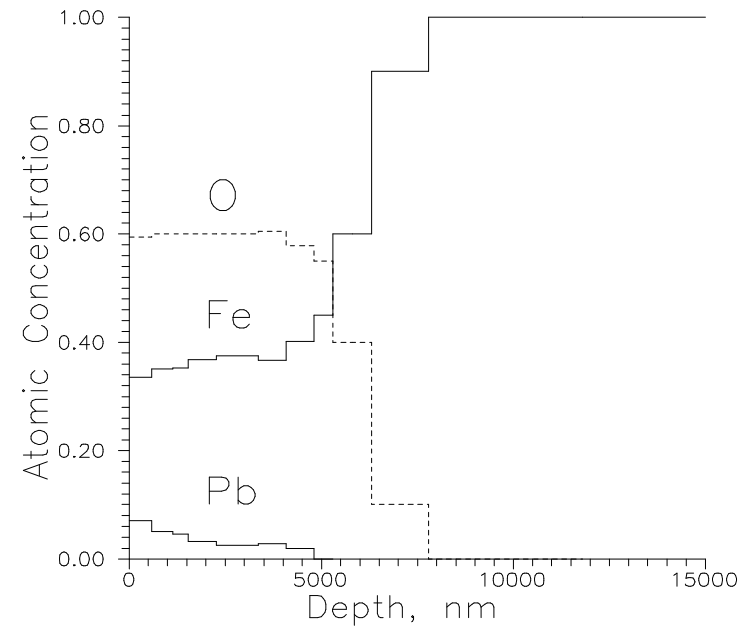
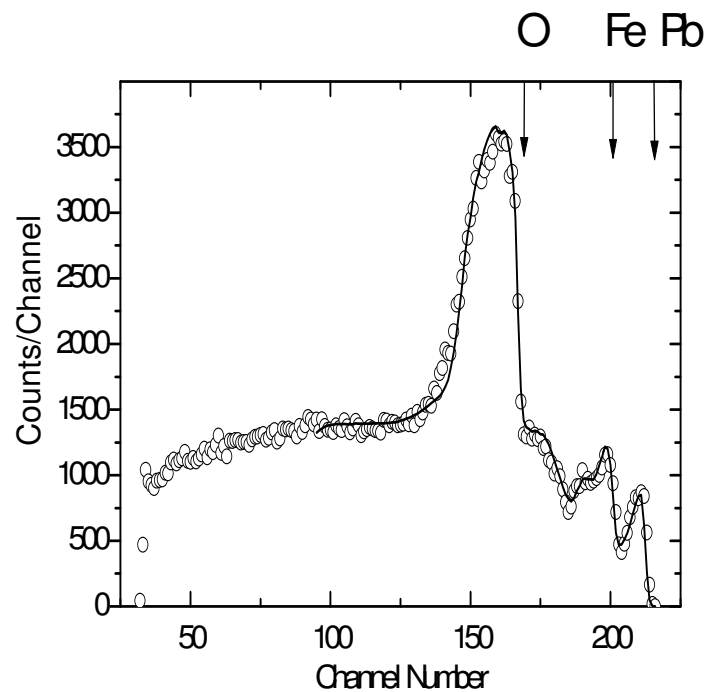
Most important in-situ results by IPPE

1. The effect of ionizing component of irradiation on the mobility of dislocations has been demonstrated for vanadium, zirconium and chromium-nickel alloys.
2. Experimental results and modeling of the periodic strain effect on radiation-induced recrystallization of ceramics (BN). It has been shown that an increased strain range accelerates the radiation-induced recrystallization.
3. Effects of macroscopic and microscopic electrical charging on the optical properties of insulators under ion irradiation have been demonstrated.
4. Correlations between mechanical, electrical and optical properties of insulators during irradiation have been found and investigated.

Nuclear micro-analysis of the materials composition and structure

- Light impurities (boron, nitrogen, oxygen) in carbon samples
- Heavy impurities in semiconductor engineering materials
- Reactor materials corrosion –
 - mass transfer of the main components of structural alloyed steels (Fe, Cr, Ni),
 - nonmetallic interstitial impurities (C, N, O),
 - alloy additions (Mo, Nb),
 - elements of liquid metal coolants (Li, Na, K, Pb, Bi)
- Dynamics of oxide film growth on the structural steel surface in water vapor and the change of the film stoichiometrics in the process of oxidation
- Other materials

The Ion Beam Analysis of the composition and structure of the oxide film formed on the steel surface bordering upon the heavy metal coolant. The elastic backscattering spectrum from a typical sample (left) and the depth profiles of oxygen, iron and lead/bismuth derived from the spectrum (right).

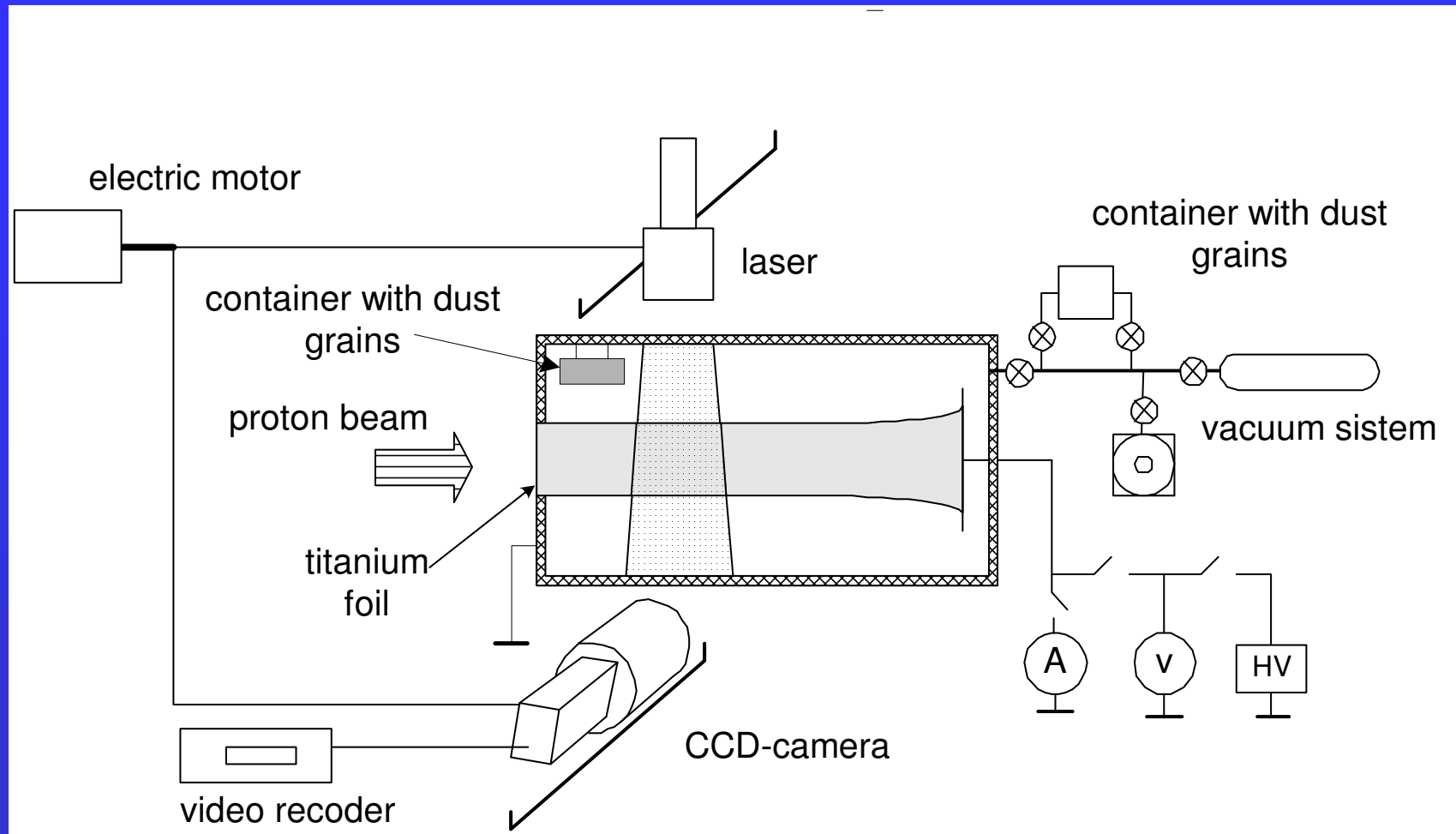


Fundamental studies in the area of dust plasma physics

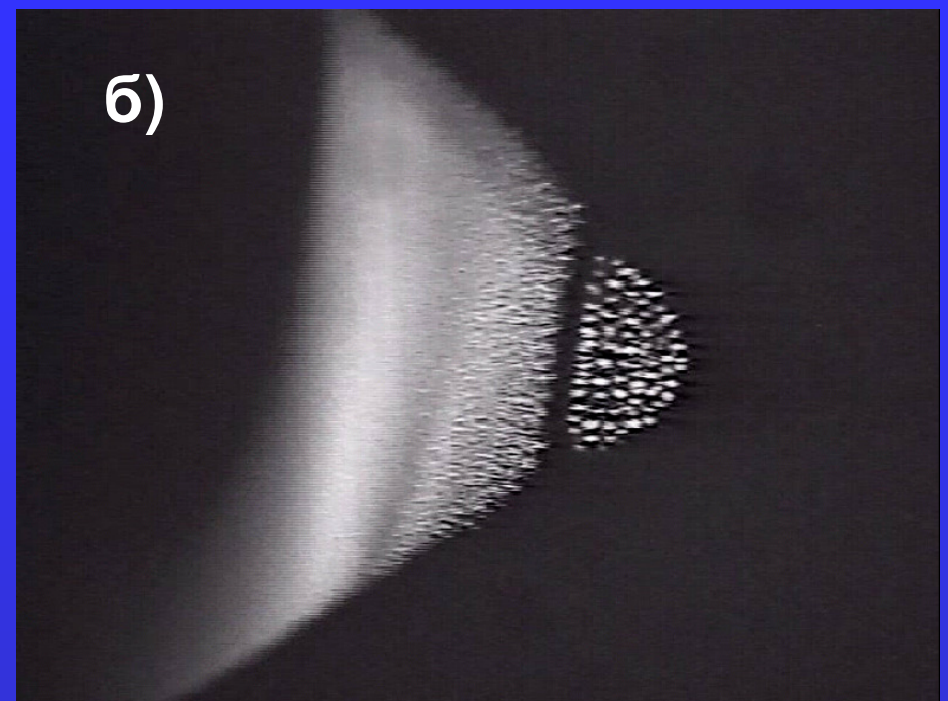
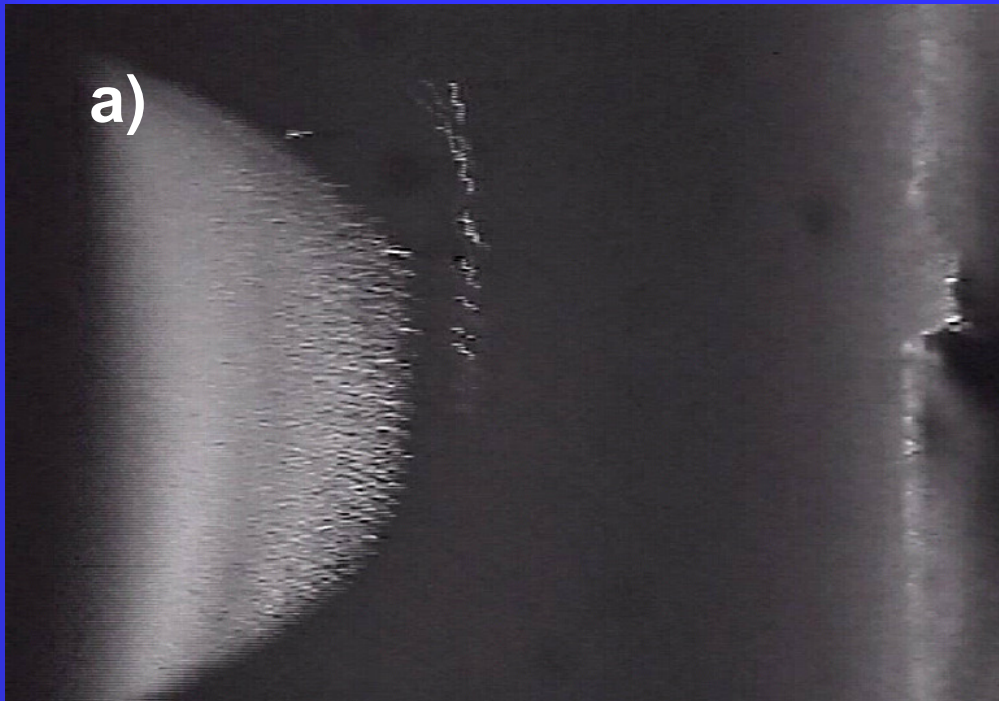
The nuclear-excited dust plasma is a new state of matter formed by the plasma particles, neutral particles, and macroscopic solid particles that have concentration high enough for the potential interaction energy between them could exceed their thermal energy owing to the charge with plasma particles.

The world's first experiments with dust particles in plasma created by proton beams were carried out at SSC RF-IPPE.

The experiments were carried out on electrostatic accelerator EG-2.5. Mono-disperse particles from melamine-formaldehyde with different radiuses from $0.5\ \mu\text{m}$ to $2.75\ \mu\text{m}$ were used in the experiments. Different inert gases (He, Ne, Ar, Xe, Kr) were used as the buffer gas in the experiments.



Dust plasma crystal



- a) *Dust structure formation: gas – krypton, gas pressure – 1 Torr, particle size - 3 μm , voltage on the electrode – 140V, the beam current – 3 μA .*
- b) *Dust crystal. Frame size 6 \times 8 mm².*

Development of membrane technologies



The main characteristics of track membranes obtained are as follows:

- film thickness 8 - 12 μm
- pore density $10^5 - 10^9 \text{ cm}^{-2}$
- pore diameter from 0.03 to 5 μm
- angular distribution of pores: isotropic in one plane
- the pore form is cylindrical and cone-shaped
- the working surface is with cone-shaped pores: porosity 1 - 3 %, diameter (0.03 - 0.12) μm
- the opposite side of this membrane: porosity 20 - 25 %, pore diameter 0.2 - 1.0 μm

Irradiation complex at EGP-15

The track membranes obtained can be used in different devices: filters for water purification, analytical track membranes for microbiological monitoring of water and air, analytical track membranes for the parasitological monitoring, primarily that of freshwater, the «breathing» packages of food products, the composite track membranes with sterilizing filtering effect for medicine, bio-technology, pharmaceutical industry

Conclusions

As a result of the development of accelerator-based technology at the IPPE, the possibilities of unique currently operating complex of electrostatic accelerators have been significantly extended.

Potentials of the complex which provides ion beams of wide mass ranges with energies from 0.1 MeV to 65 MeV and is equipped with work stations for the experimental research, cover a wide scope of applied and fundamental research on emergent problems of nuclear science and technology

XVIII International Conference on
Electrostatic Accelerators and Beam
Technologies
(ESACCEL 2010)



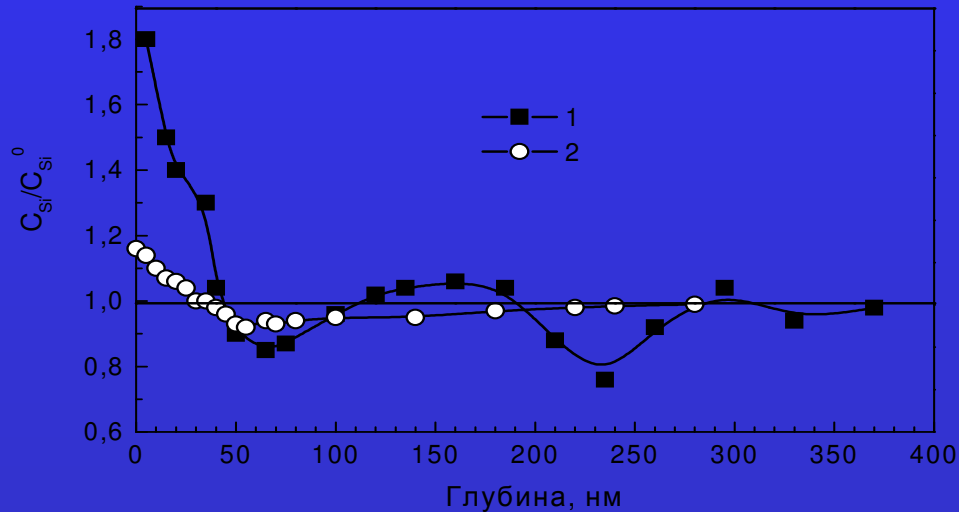
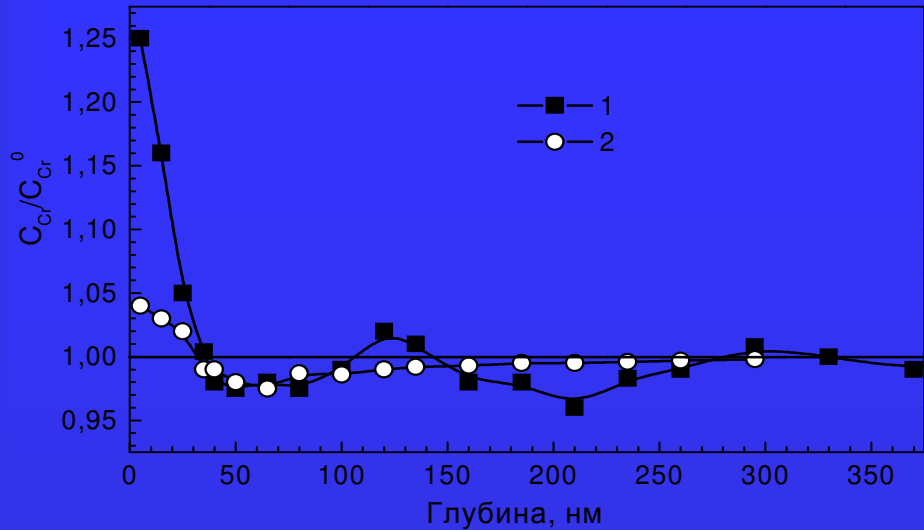
Obninsk, Russia
October 2010

THANK YOU FOR ATTENTION!





RIS in EP-823



Ferritic-martensitic steel EP-823 (0.16C-12Cr-Mo-W-Si-V-Nb-B) was irradiated with 7 MeV Ni⁺⁺ ions at **EGP -15** (penetration depth ~ 1400 nm, uniform damage rate near the surface) and with 70 keV He⁺ ions at **ILU -100** (penetration depth ~ 240 nm, nonuniform damage rate near the surface) at the temperature of 500°C.

Using the method of x-ray photoelectron spectroscopy profiles of the radiation-induced segregation of chromium and silicon near the target surface were measured in irradiated samples
1 - He⁺, 2×10^{20} ion/m² (0.2 dpa);
2 - Ni⁺⁺, 6×10^{18} ion/m² (0.2 dpa)

IPPE ACTIVITIES ON THE THEORY AND MODELLING OF MICROSTRUCTURE AND PHASE CHANGES IN METALLIC MATERIALS UNDER IRRADIATION

1. Mechanisms of point defect clusters formation in metals and the dilute alloys under irradiation

- *Development of the theory of interstitial dislocation loop formation in metals and dilute alloys at the initial stage of electron irradiation*
- *Development of the theory of voids and interstitial loops formation under steady state conditions*

2. Development of the theory and modelling of radiation-induced segregation of base and alloying chemical elements in substitutional alloys

- *Analytical expressions for steady state profiles of alloy components near point defect sinks*
- *Combined radiation-induced segregation and thermal adsorption at grain boundaries in multicomponent alloys*
- *Modeling of non-stationary radiation-induced segregation of base and alloying components in binary and ternary alloys*
- *Influence of the radiation-induced segregation on phase structure and swelling of alloys*

3. Theoretical modelling of radiation effects

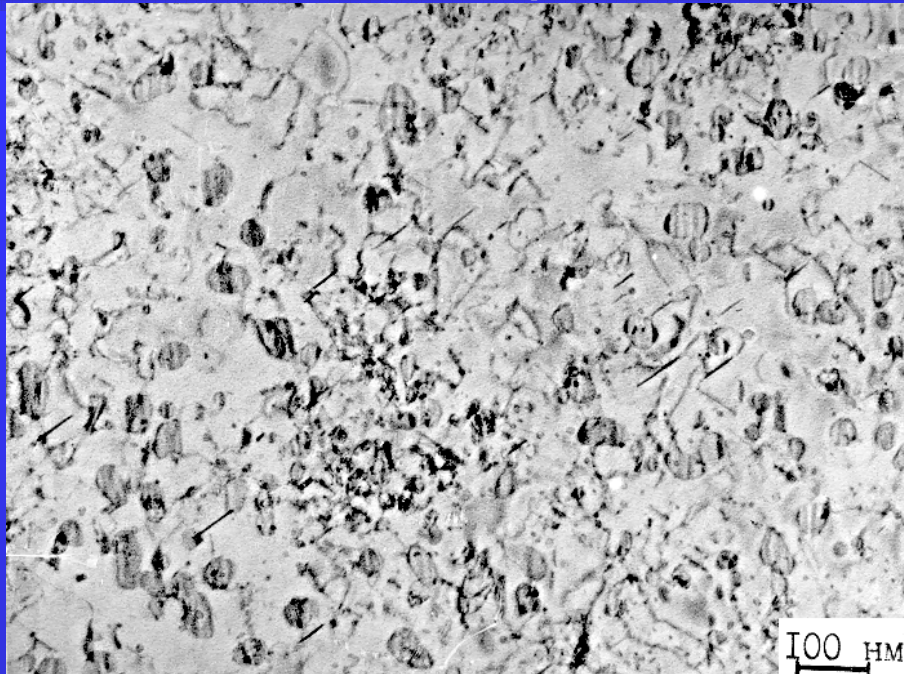
- *Analytical model of phase layer growth at the surface of an under-saturated binary alloy under irradiation*
- *Void swelling in metals and alloys*
- *Irradiation embrittlement of VVER pressure vessel steels*

4. Development of molecular dynamics methods and calculation of properties of point defects and point defect clusters in metallic materials

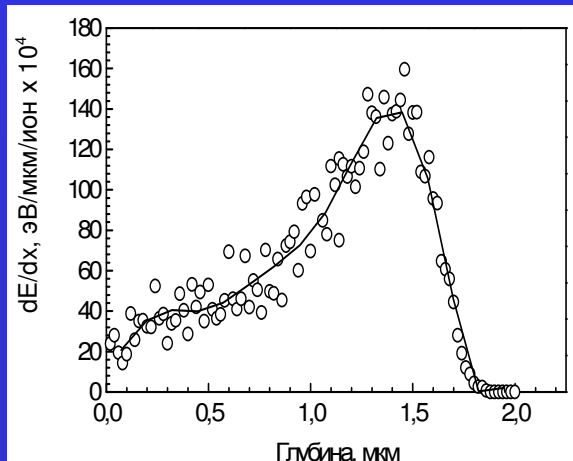
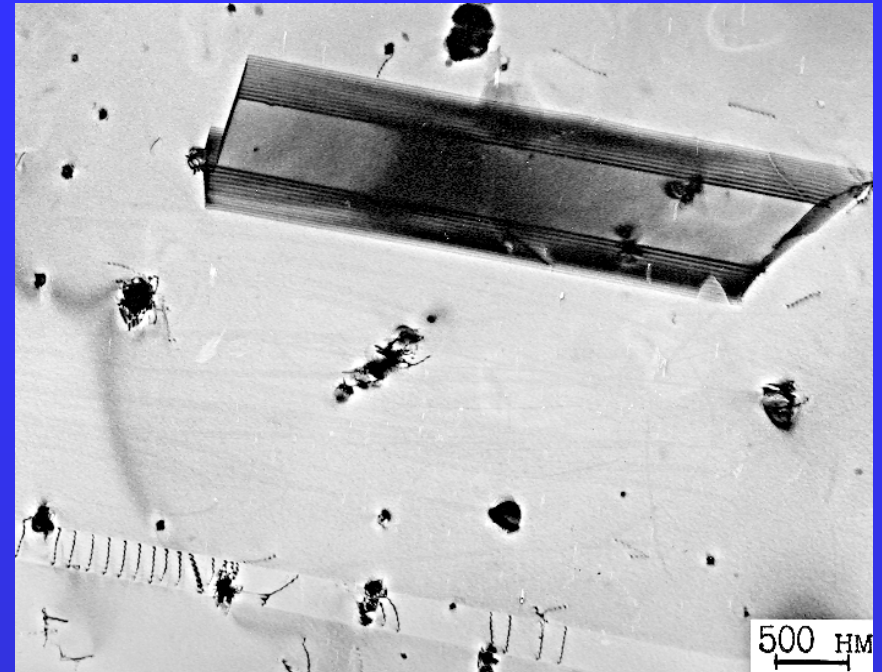
- *Derivation of interatomic interaction potentials for transition metals (Fe, Cr) with an account of magnetic interaction*
- *Molecular dynamics and ab initio calculations of structures, energy and diffusion characteristics of point defects and point defect clusters in metals (Fe, Ni) and Fe-Cr alloys*

Irradiation of Russian steel (X18H9T) on accelerator EGP-15

Dislocation loops in steel irradiated with ions (Ni²⁺) at 7.5 MeV energy at temperature of 550 C, ~10 dpa



Micro-structure of steel before irradiation



Distribution of radiation damages over the steel sample depth under ion irradiation (Ni²⁺) at 7.5 MeV energy

Ion Beams (energy of 3 - 60 MeV; ion current of 10 - 1000 nA) at the EGP-15 Tandem

Ions	Beam Current from Ion Source [μA]
H ⁻	10 - 20
D ⁻	20 - 40
He ⁻	0,5 - 2
Li ⁻	0,5 - 1,5
B ⁻	1 - 2
C ⁻	40 - 80
(CN) ⁻	1 - 5
O ⁻	20 - 50
F ⁻	10 - 20
Al ⁻	0,5 - 1
Si ⁻	20 - 50

Ions	Beam Current from Ion Source [μA]
P ⁻	5 - 20
Cl ⁻	4 - 20
Ti ⁻	2 - 6
(Cr) ⁻	1 - 4
(FeO) ⁻	1 - 5
Ni ⁻	10 - 20
Cu ⁻	5 - 15
(ZnO) ⁻	0,5 - 2
Ge ⁻	3 - 10
As ⁻	5 - 10

Ions	Beam Current from Ion Source [μA]
Se ⁻	3 - 12
Br ⁻	10 - 20
(NbC) ⁻	0,5 - 1
Ag ⁻	2 - 3
Sn ⁻	1 - 3
I ⁻	10 - 30
Pt ⁻	15 - 20
Au ⁻	30 - 50

The oxygen and silicon depth profiles obtained by Ion Beam Analysis for the steel surface tested in the heavy metal coolant flow

